

Geostrophic balance of the equatorial zonal flow

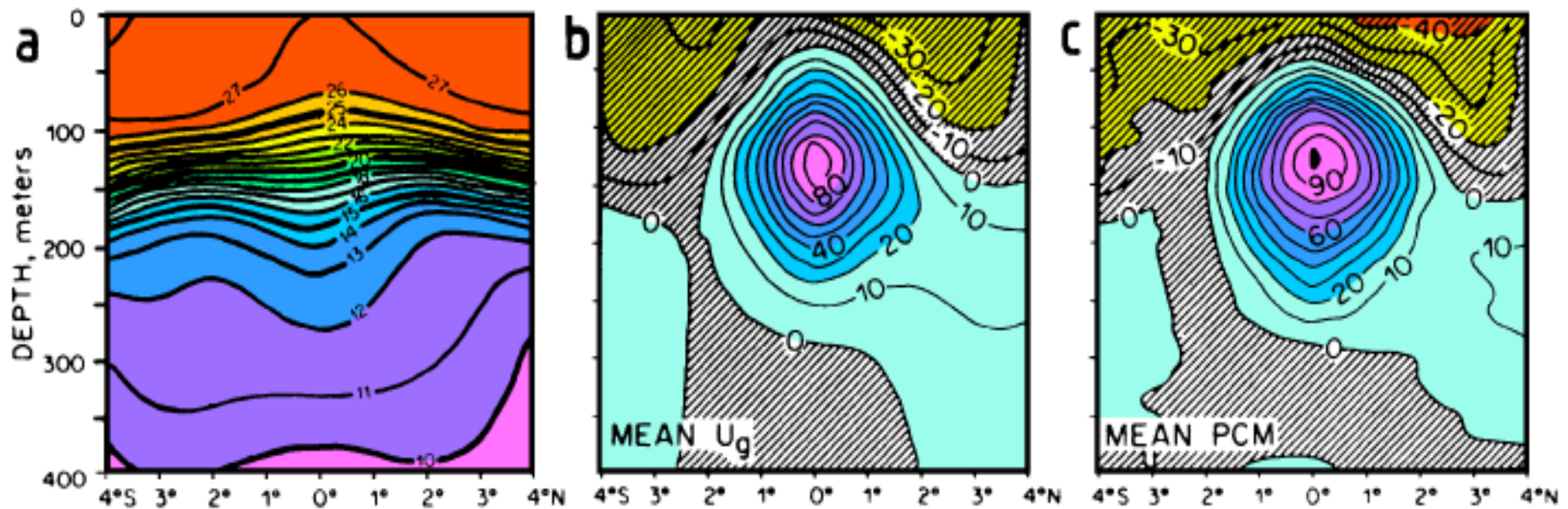


Fig. 8.8. The Equatorial Undercurrent during February 1979 - June 1980 near 155°W . (a) Mean temperature ($^\circ\text{C}$), (b) mean geostrophic zonal velocity (10^{-2} m s^{-1}), (c) mean observed zonal velocity (10^{-2} m s^{-1}). Note the spreading of the isotherms at the equator. From Lukas and Firing (1984).

The Stommel model: transition from Ekman balance to non-rotational physics on the equator

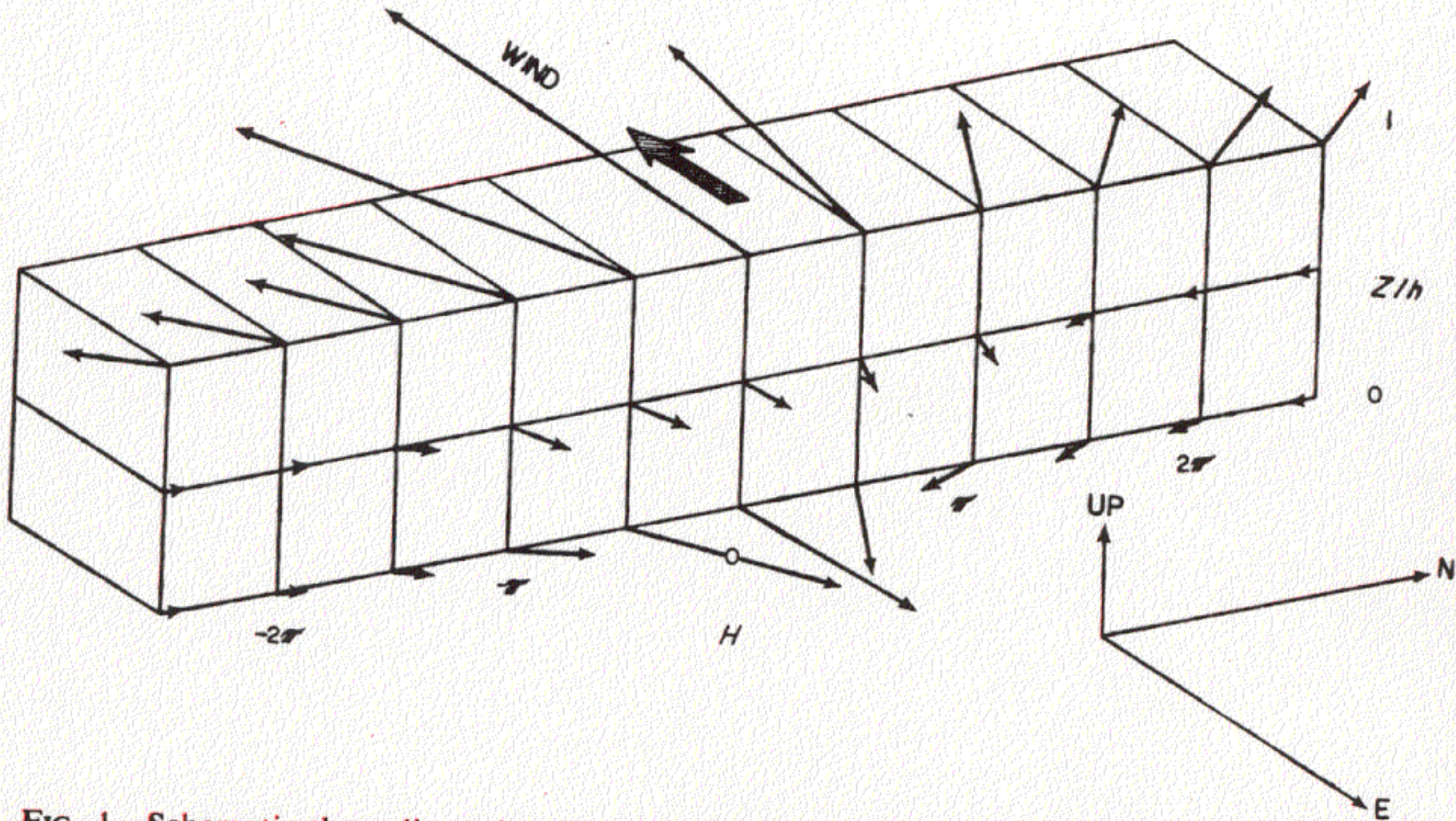
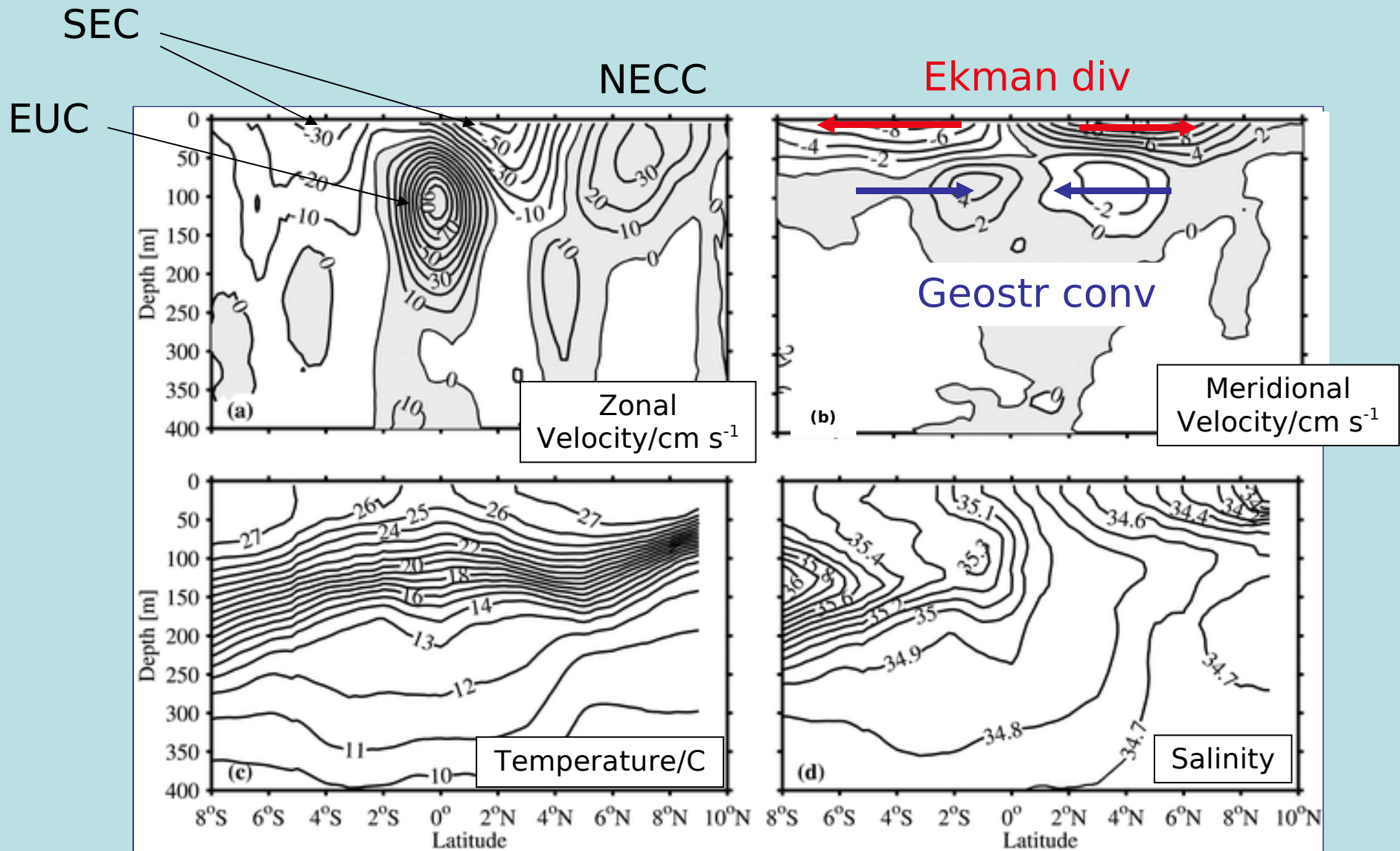


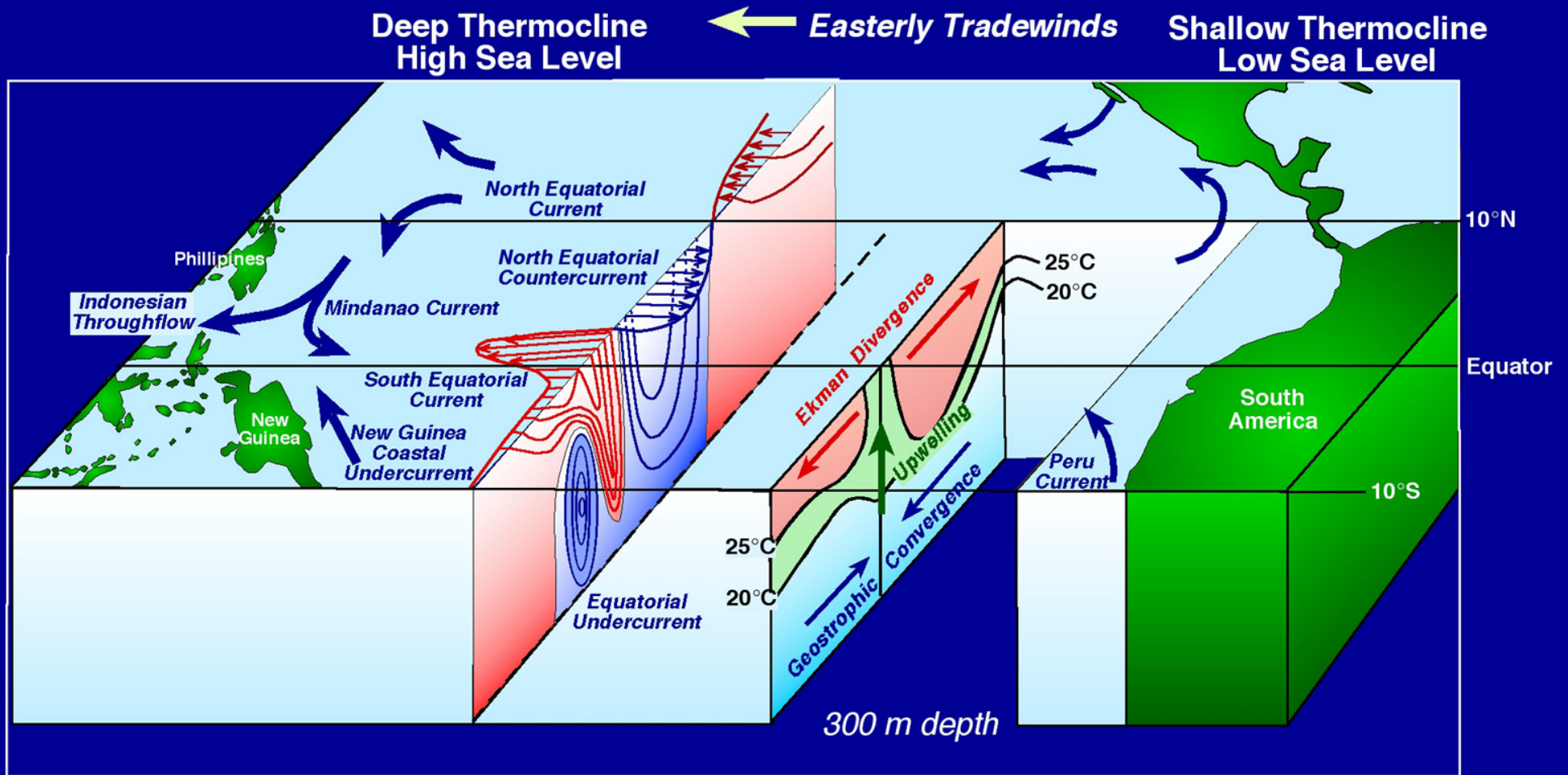
FIG. 1. Schematic three-dimensional diagram of the combined frictional and geostrophic flow field in the neighbourhood of the equator, not showing the vertical component of velocity (which can in principle be determined from continuity).

Stommel, 1959, DSR., 6, 298-302

Meridional Structure, 136°W



Ocean Circulation Schematic



After Philander, 1990

Complex vertical structure of flow even at great depth

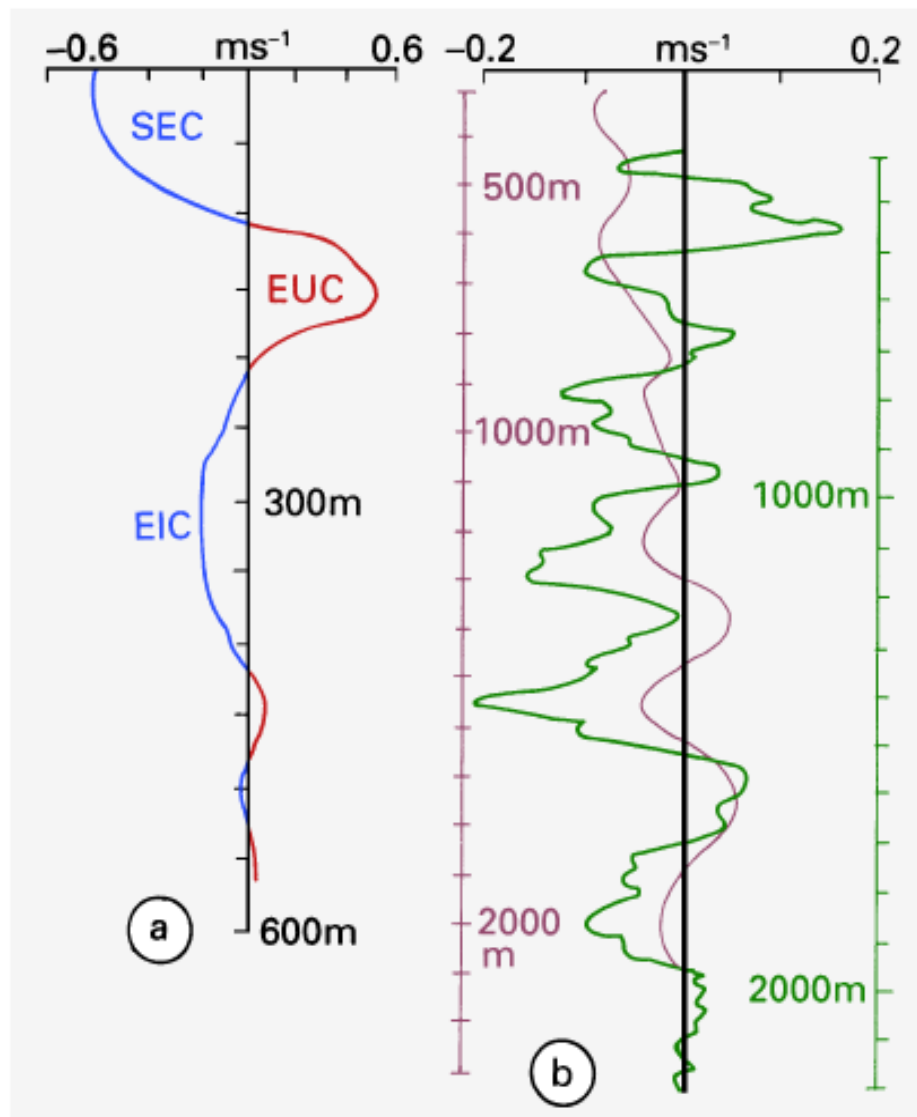


Fig. 8.15. Evidence for banded structure of currents at the equator.

(a) The South Equatorial Current (SEC), Equatorial Undercurrent (EUC), and Equatorial Intermediate Current (EIC) at 165°E;

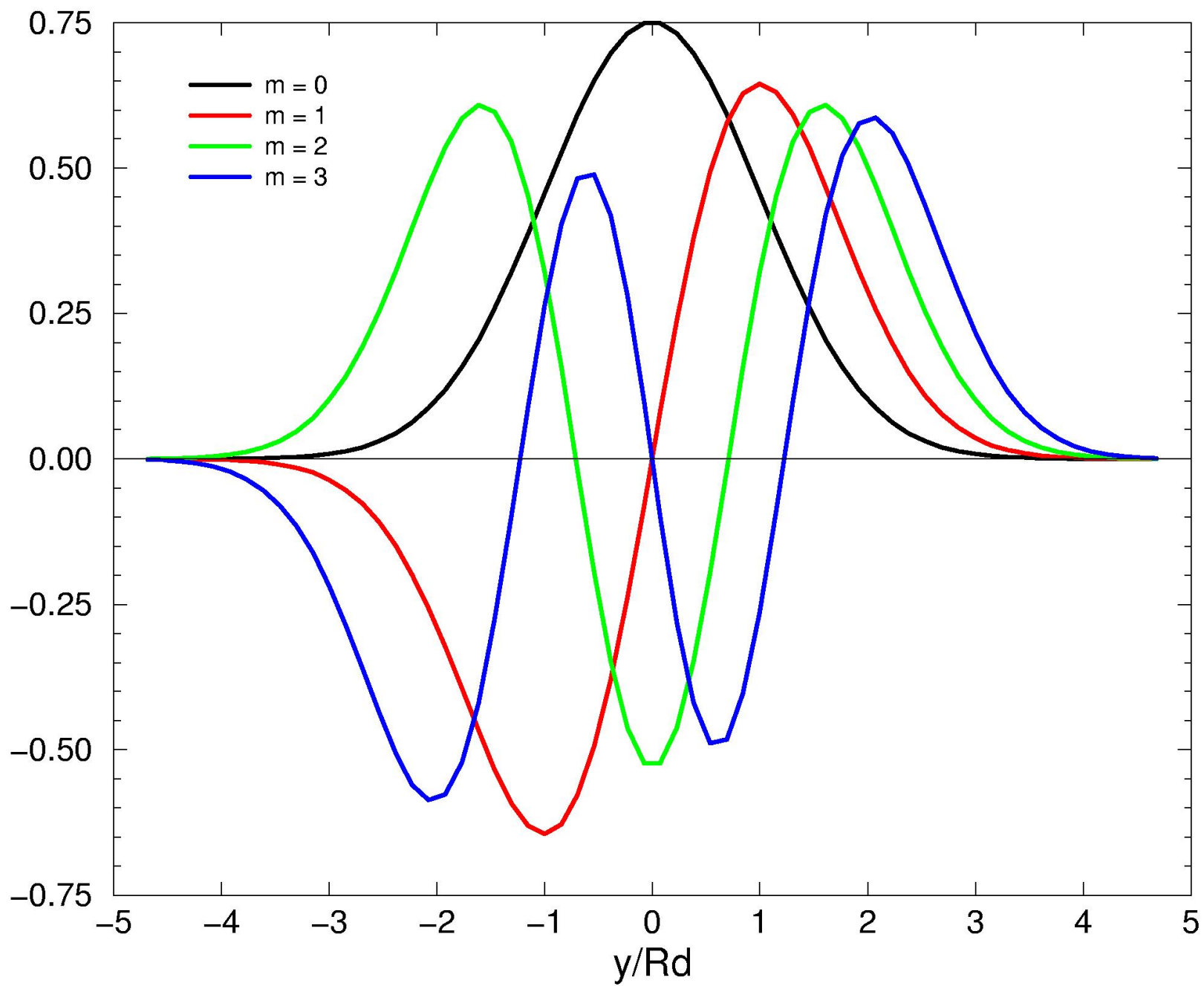
(b) deep equatorial currents at 150 - 160°W during 1980 (solid line, right depth scale) and during March 1982 - June 1983 (thin line, left depth scale). The cores of all current bands coincide if the entire current system during 1982/83 is shifted upward some 130 m.

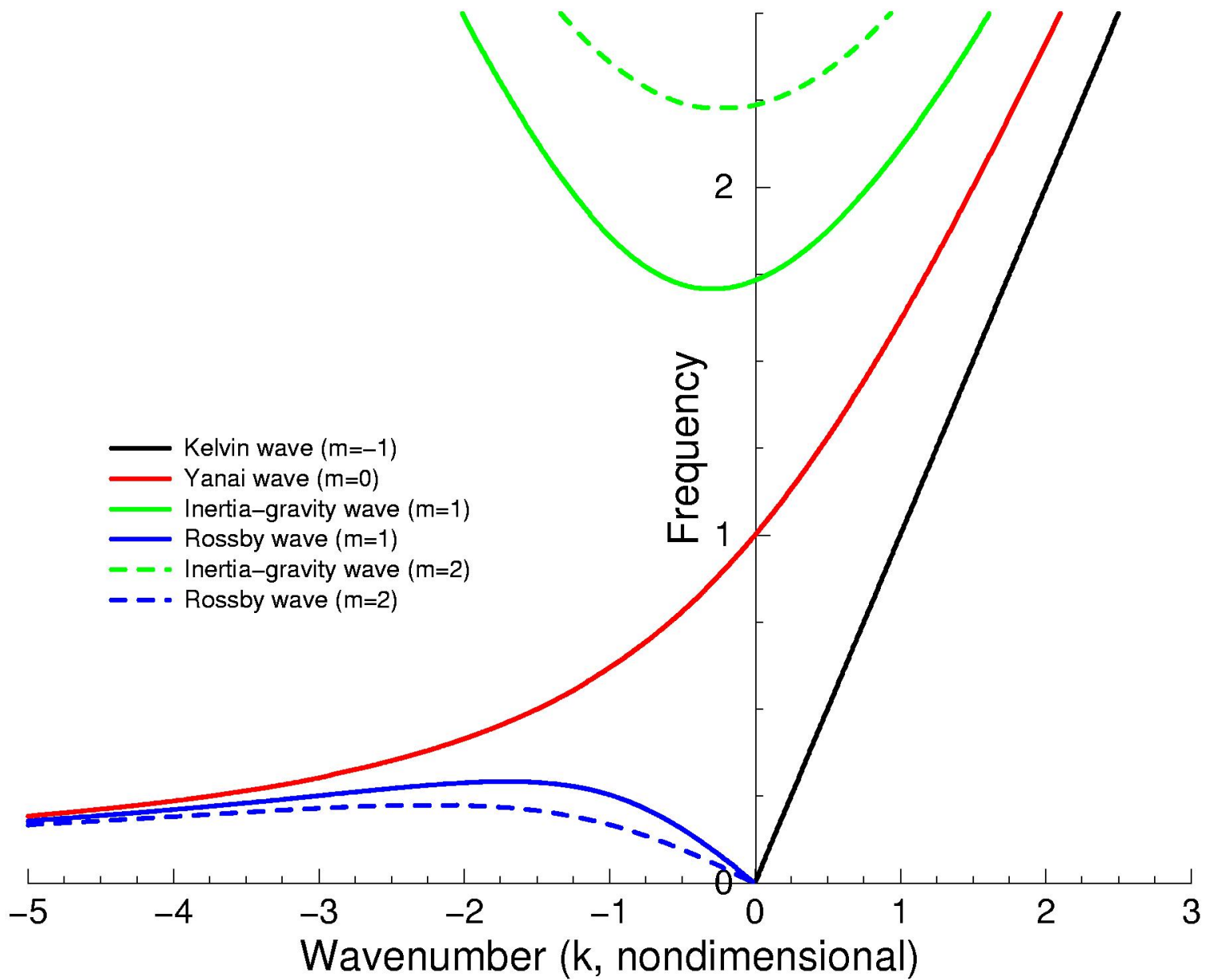
Note the different depth and velocity scales. Adapted from Delcroix and Henin (1988) and Firing (1987).

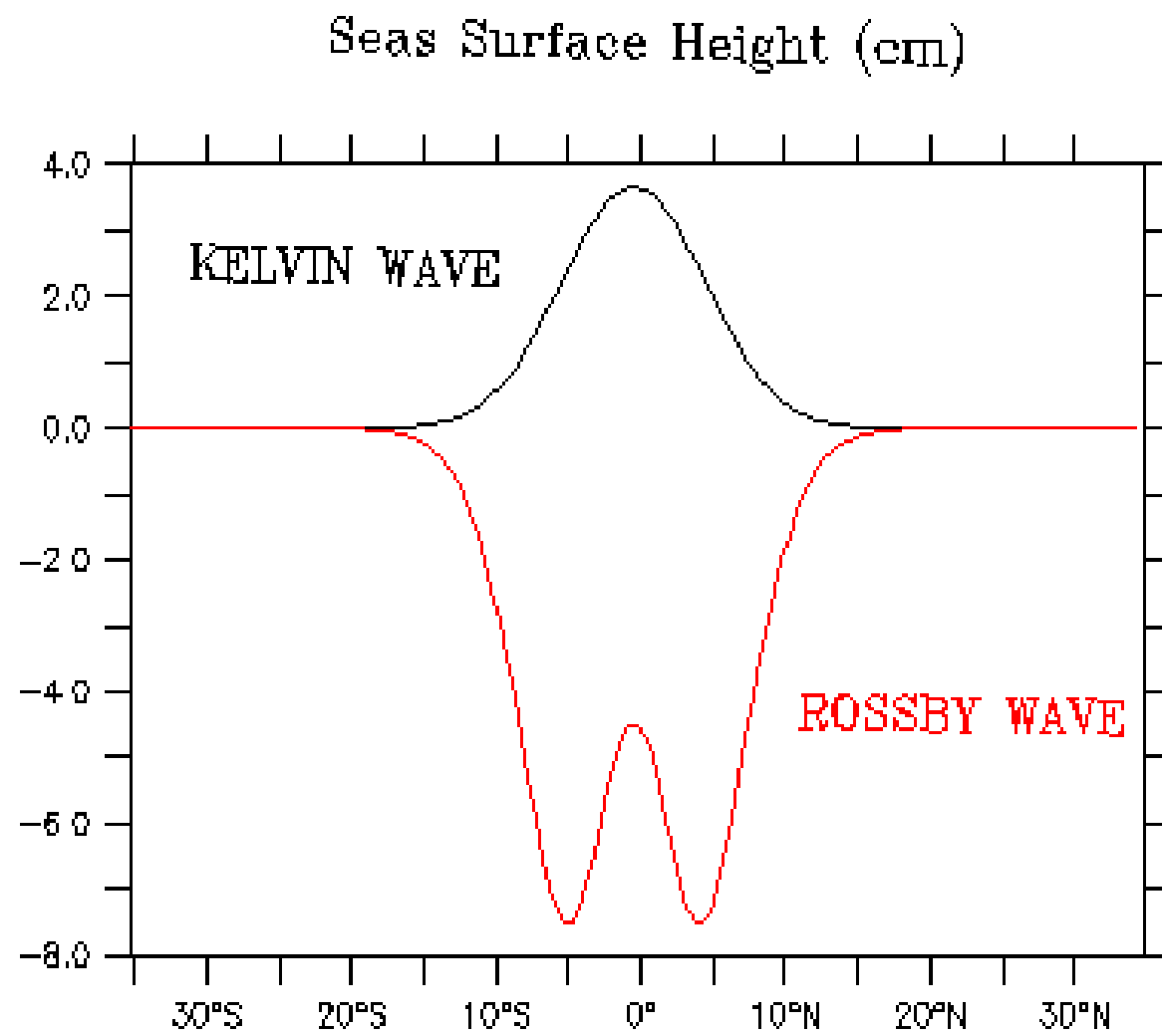
Eastern tropical Pacific suggested reading

Kessler, W. S., 2006: The circulation of the eastern tropical Pacific: A review. *Prog. Oceanogr.*, 69, 181-217.

Willett, C. S., R. R. Leben and M.F. Lavin, 2006: Eddies and tropical instability waves in the eastern tropical Pacific: A review. *Prog. Oceanogr.*, 69, 218-238.







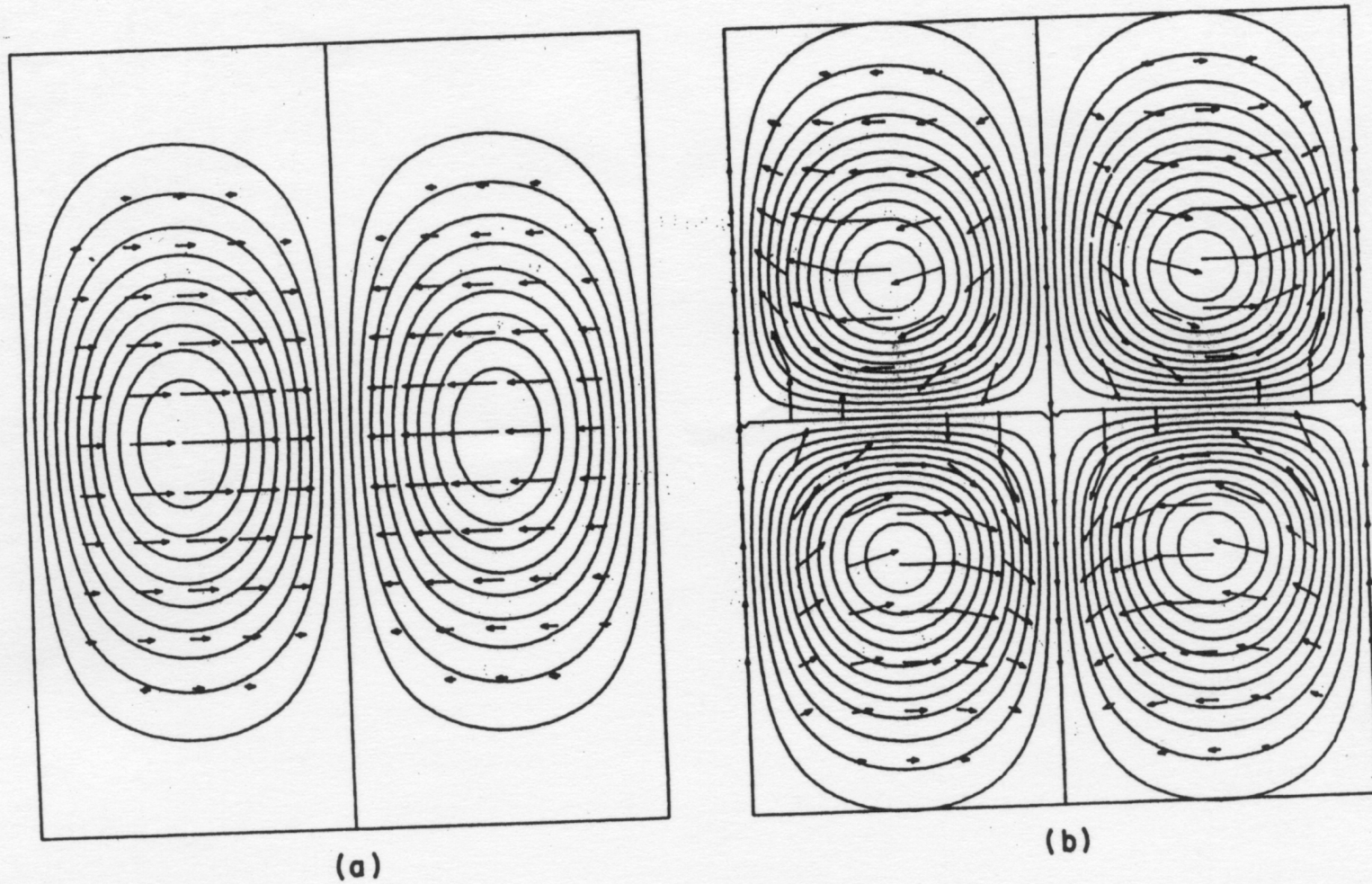
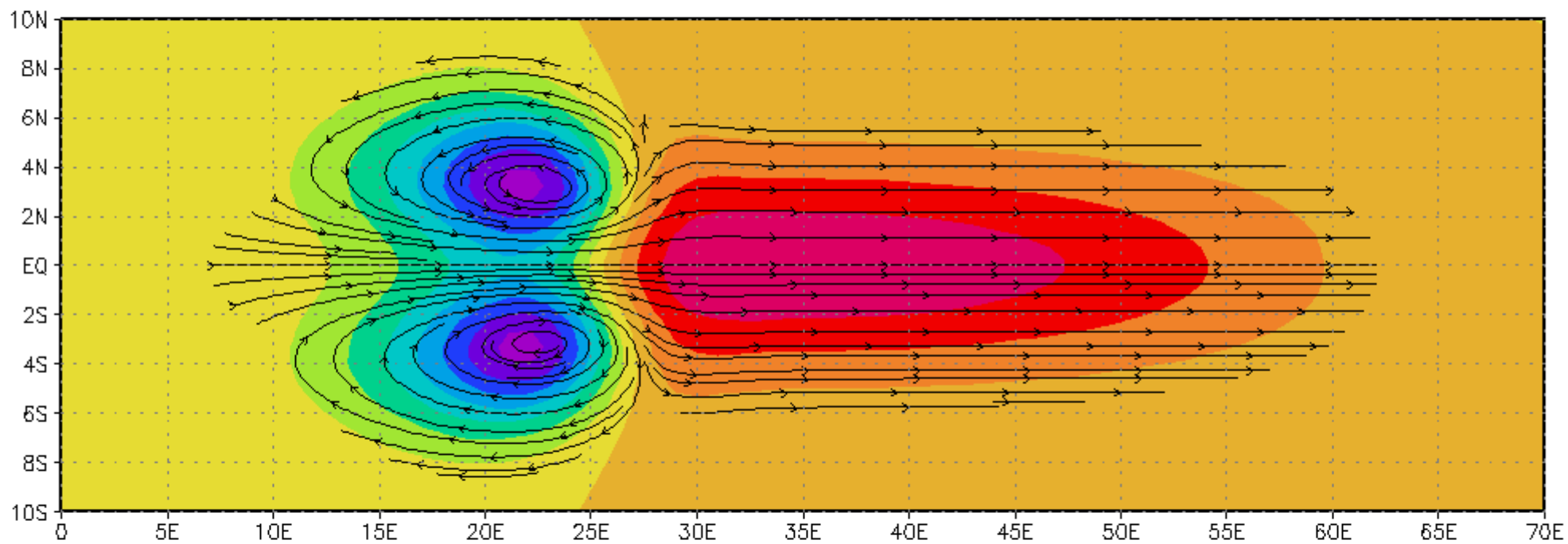
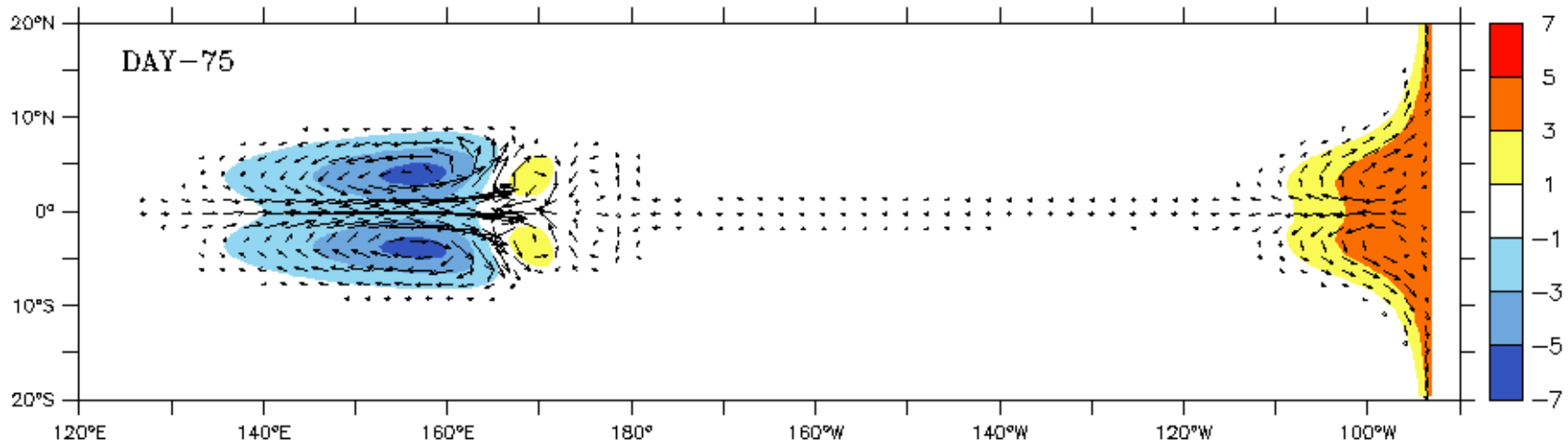
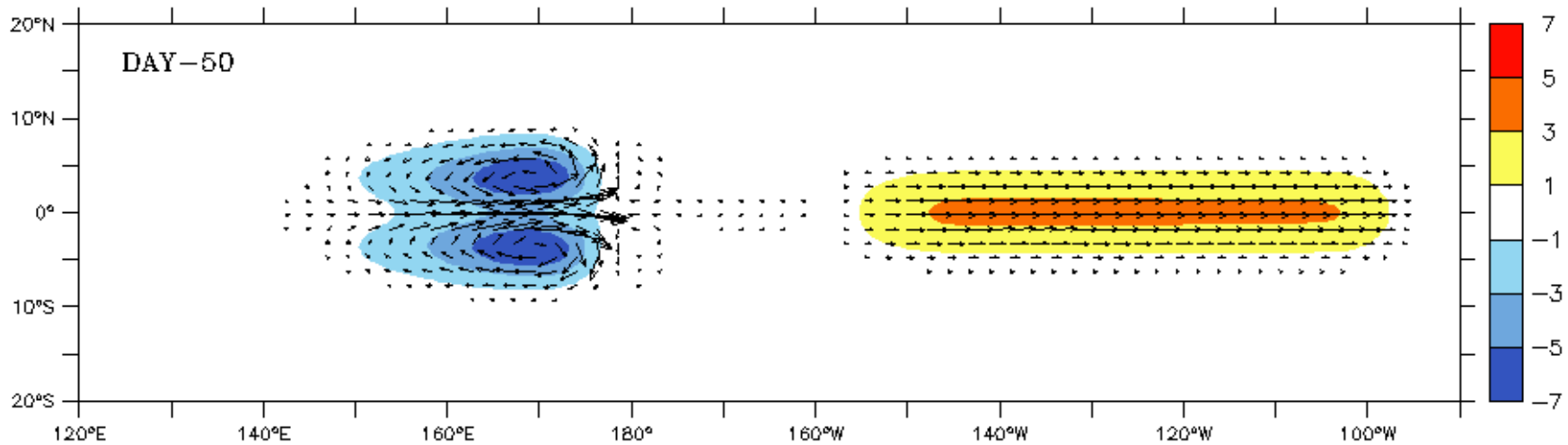
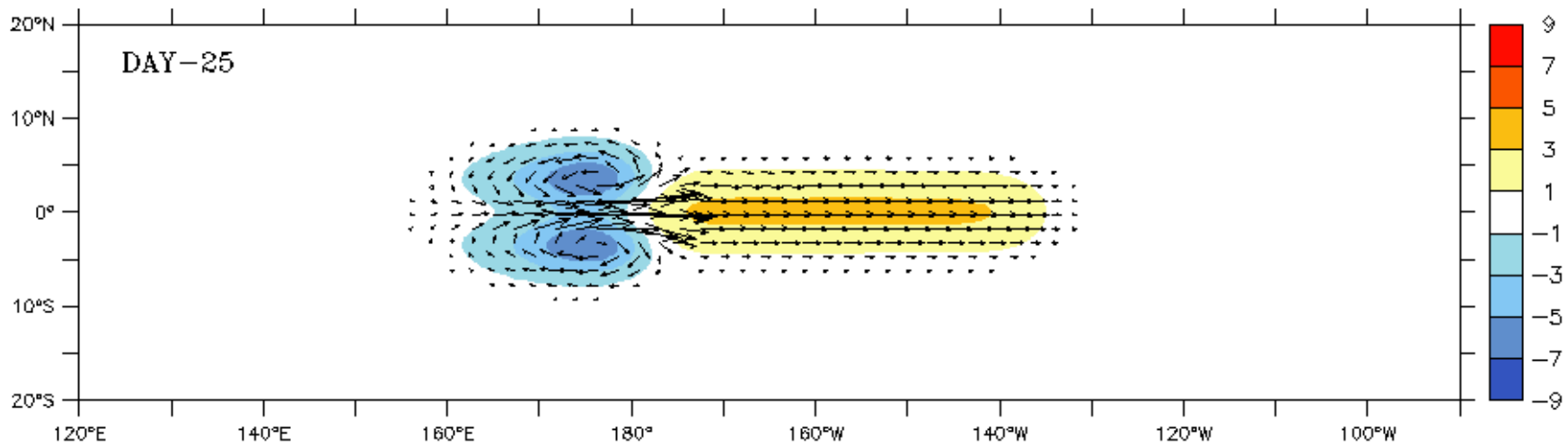
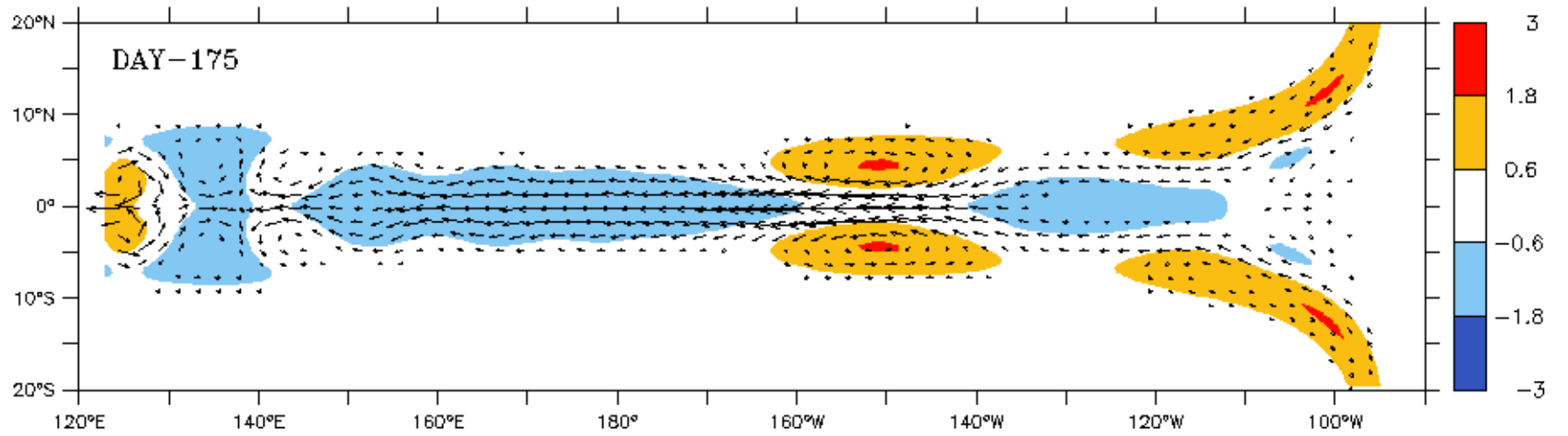
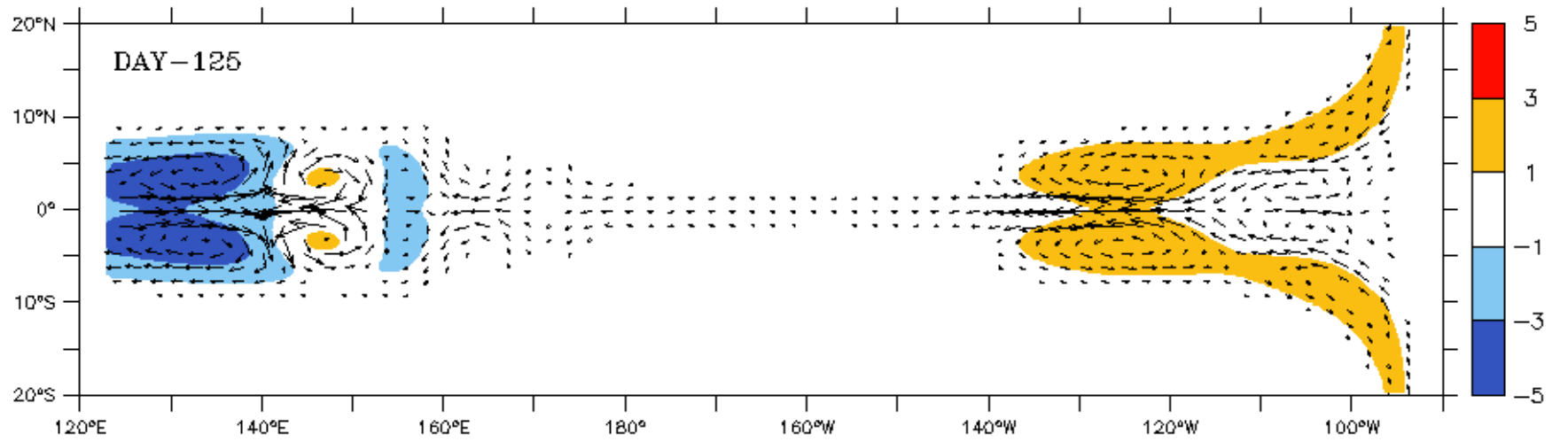
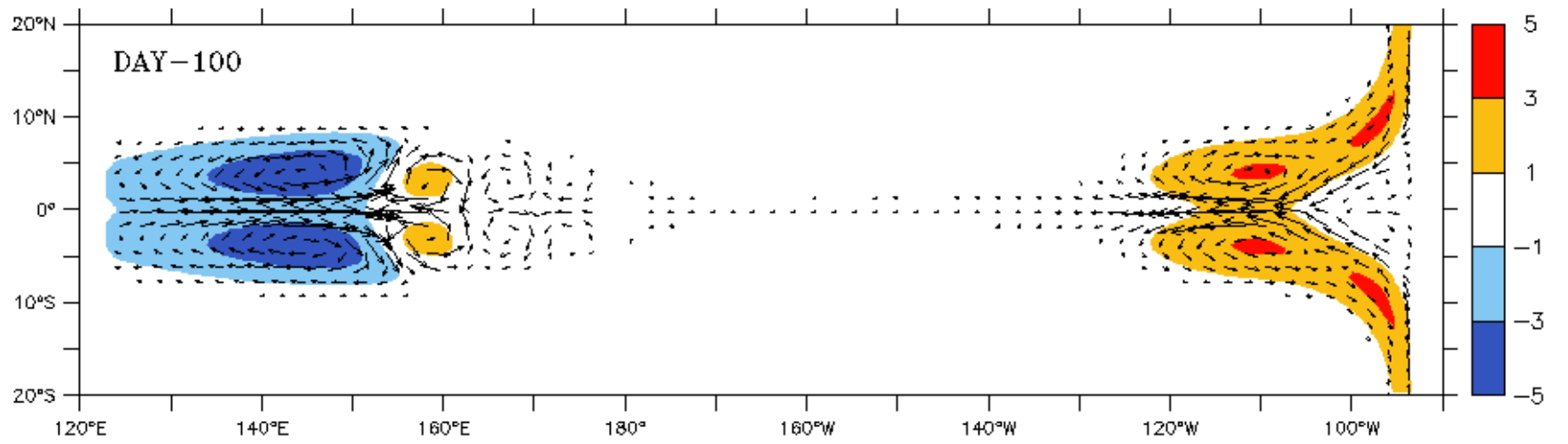


Fig. 11.2. Contours of surface elevation and arrows representing currents for (a) a Kelvin wave and (b) an eastward-propagating mixed planetary-gravity wave. Both waves have eastward phase velocity and eastward group velocity. Fluid particles move parallel to the equator in the case of the Kelvin wave and move anticyclonically around elliptical orbits in the case of the mixed wave. The figures show a range of latitudes corresponding to ± 4 equatorial Rossby radii.







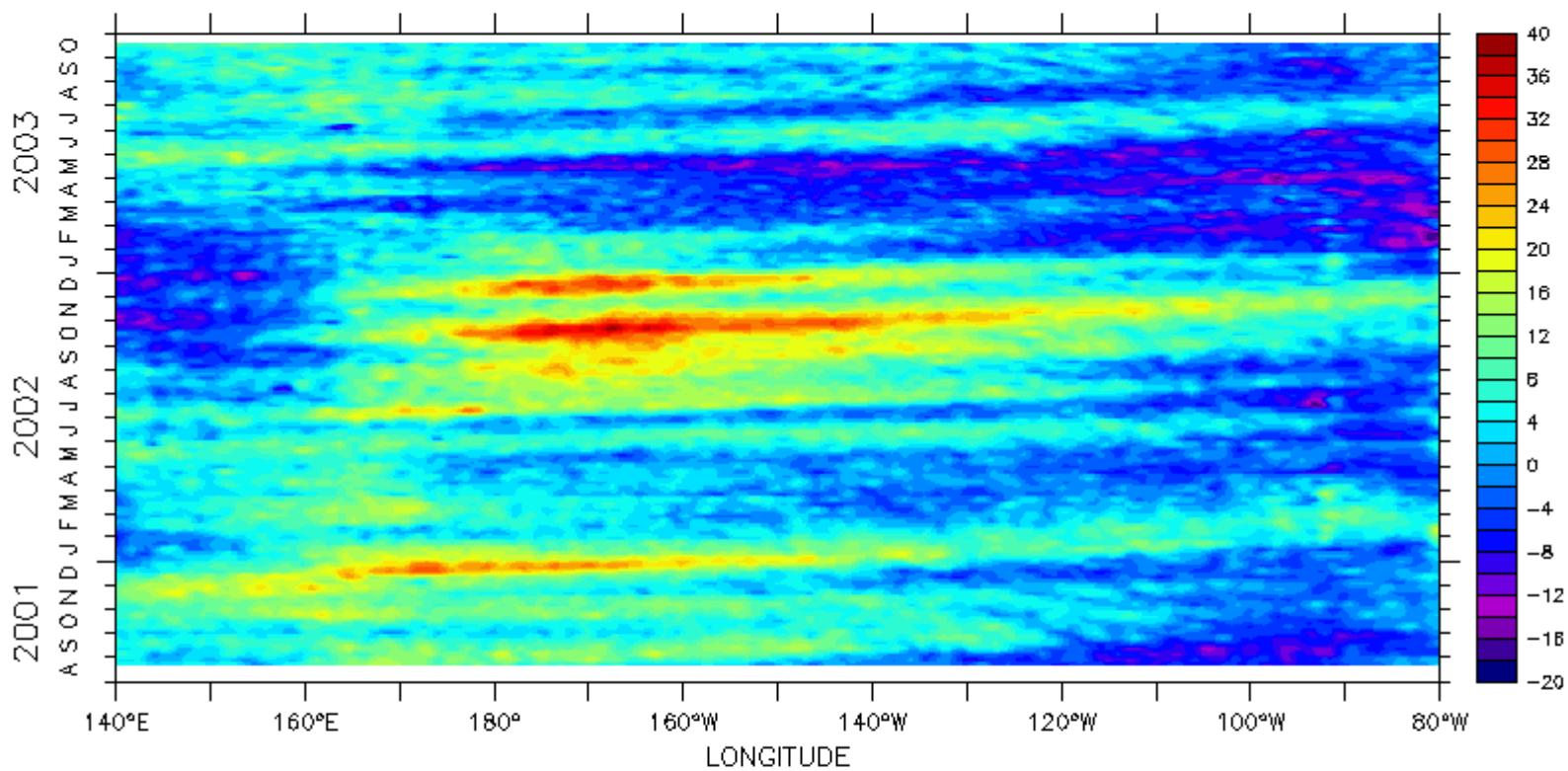


AVISO

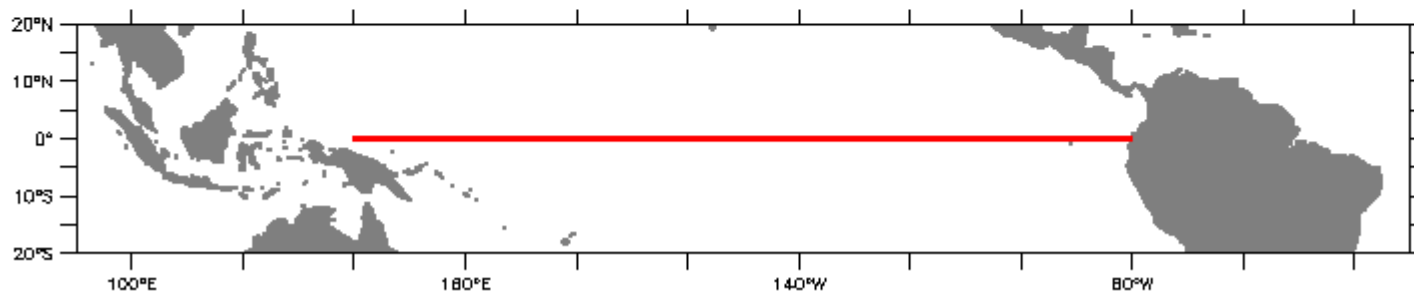
LATITUDE : 0.09S

DATA SET: msla_oer_merged_h

SSALTO/DUACS – NRT MSLA – Merged Product



H (cm)



LAS 7.+ / Ferret 6.07 NOAA / PMEL

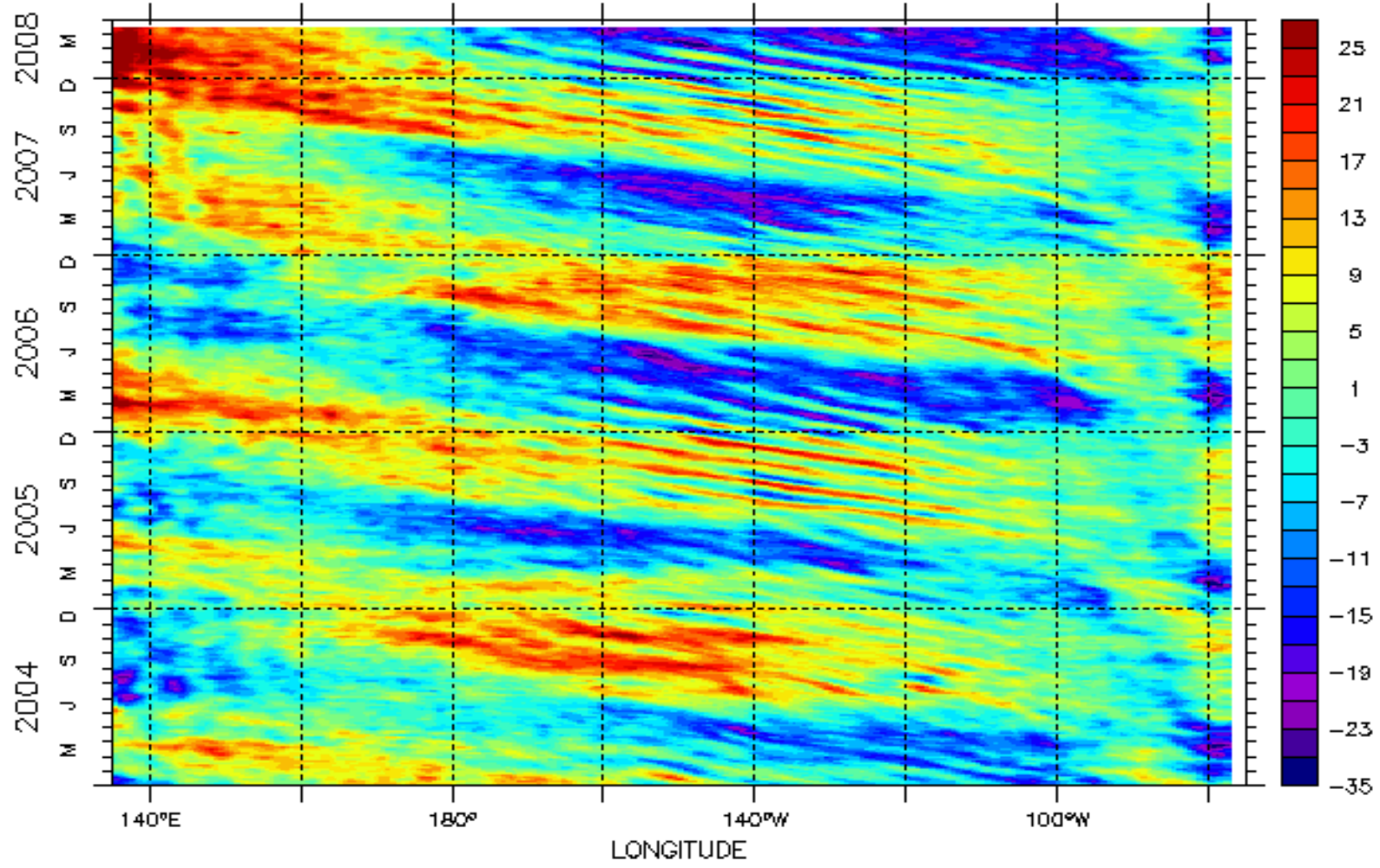
DODS URL: <http://rdp2-joune.cis.fr:8180/thredds/dodsC/>

DATA SET: duacs_global_nrt_msla_merged_h

LATITUDE : 4.9N

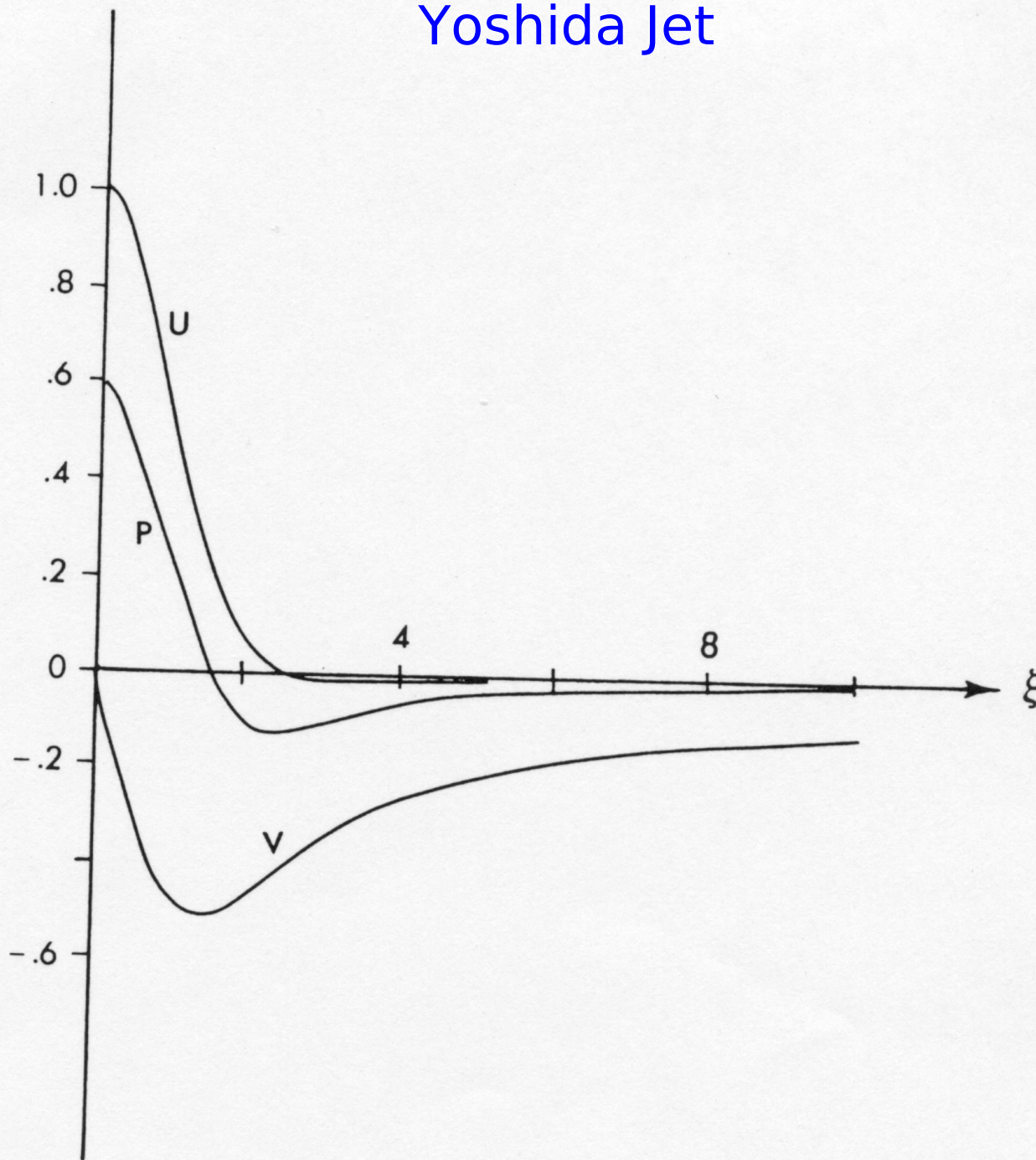
SSALTO/DUACS - NRT MSLA - Merged Product

Strided 2 in X



Maps of Sea Level Anomalies Merged (cm)

Yoshida Jet



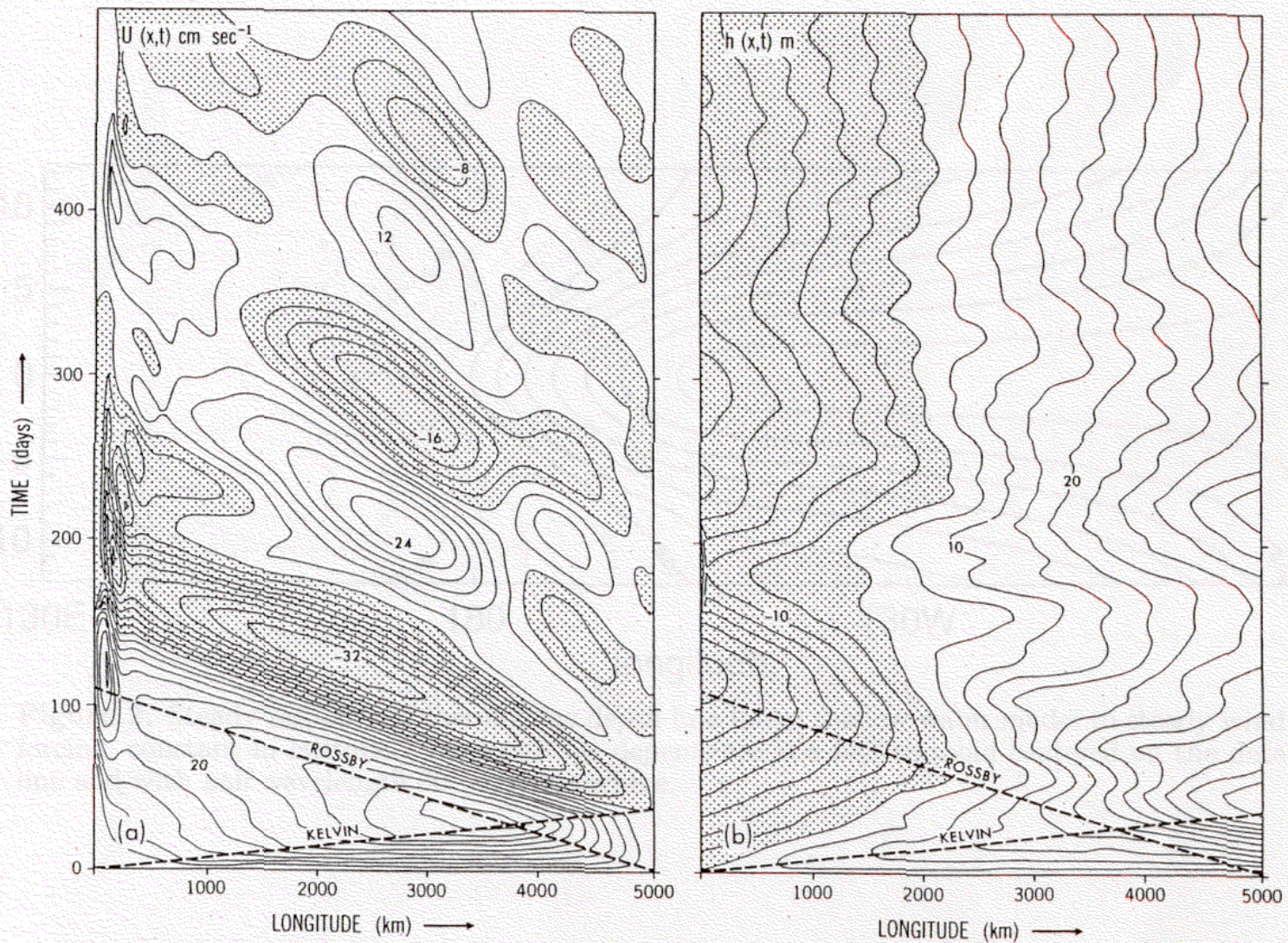


Figure 3.18. Changes in the zonal velocity component (centimeters per second) and in departures from the mean depth of the thermocline along the equator after the sudden onset of spatially uniform eastward winds. The dashed lines indicate the speeds at which Kelvin and the gravest Rossby mode propagate. The thermocline is elevated and motion is westward in shaded areas.

Philander

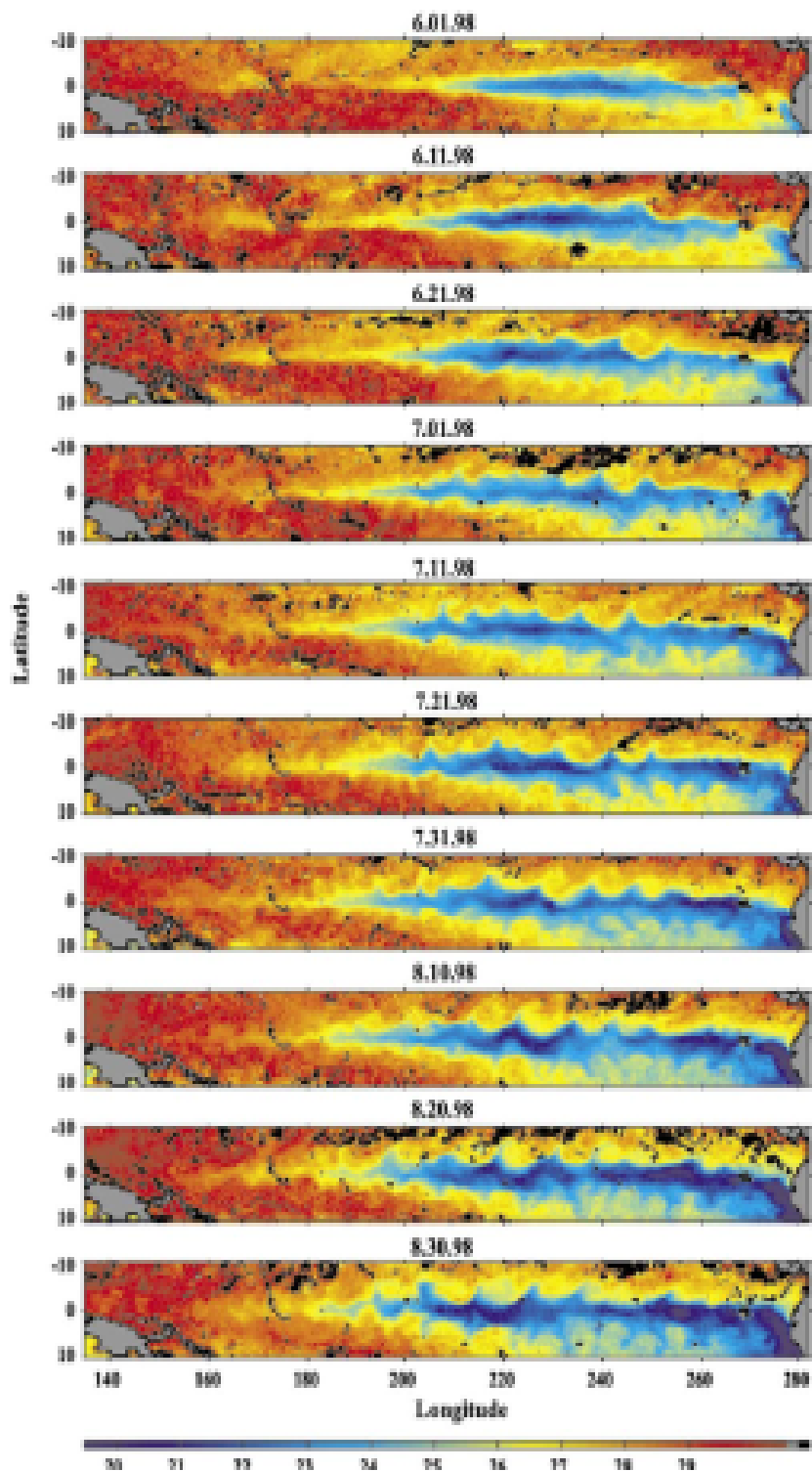


Fig. 2. Tropical instability waves (TIW) seen in imagery from the Tropical Rainfall Measuring Mission (TRMM) Microwave Imager (TMI). TMI imagery courtesy of Remote Sensing Systems (<http://www.rssmi.com/>).